




# Thermal stability, swelling and degradation behaviour of natural fibre based hybrid polymer composites

Bhabatosh Biswas · Pravin Sawai · Angshuman Santra · Amal Gain · Prosenjit Saha · Bhairab Chandra Mitra · Nil Ratan Bandyopadhyay · Arijit Sinha 

Received: 16 November 2018 / Accepted: 14 March 2019 / Published online: 20 March 2019  
© Springer Nature B.V. 2019

**Abstract** Unsaturated Polyester (UP) based composites with 5, 15, 25, 35 and 45 wt% filler content have been fabricated by compression moulding technique. The NaOH treated discontinuous jute fibre has been used along with vinyl silane treated zirconia ( $ZrO_2$ ) particle as the dispersing phases. The structures were characterized by scanning electron microscopy and Fourier transform infrared spectroscopy. The thermal stability of the UP and UP based composites

were observed using electronic thermal insulation tester, thermo-gravimetric analyser, differential scanning calorimetry and limiting oxygen index analyser. The swelling behaviour has been investigated in different solutions having a range of pH values. The optimum results were obtained with 35 wt% filler content for UP/Jute/ $ZrO_2$  composites.

---

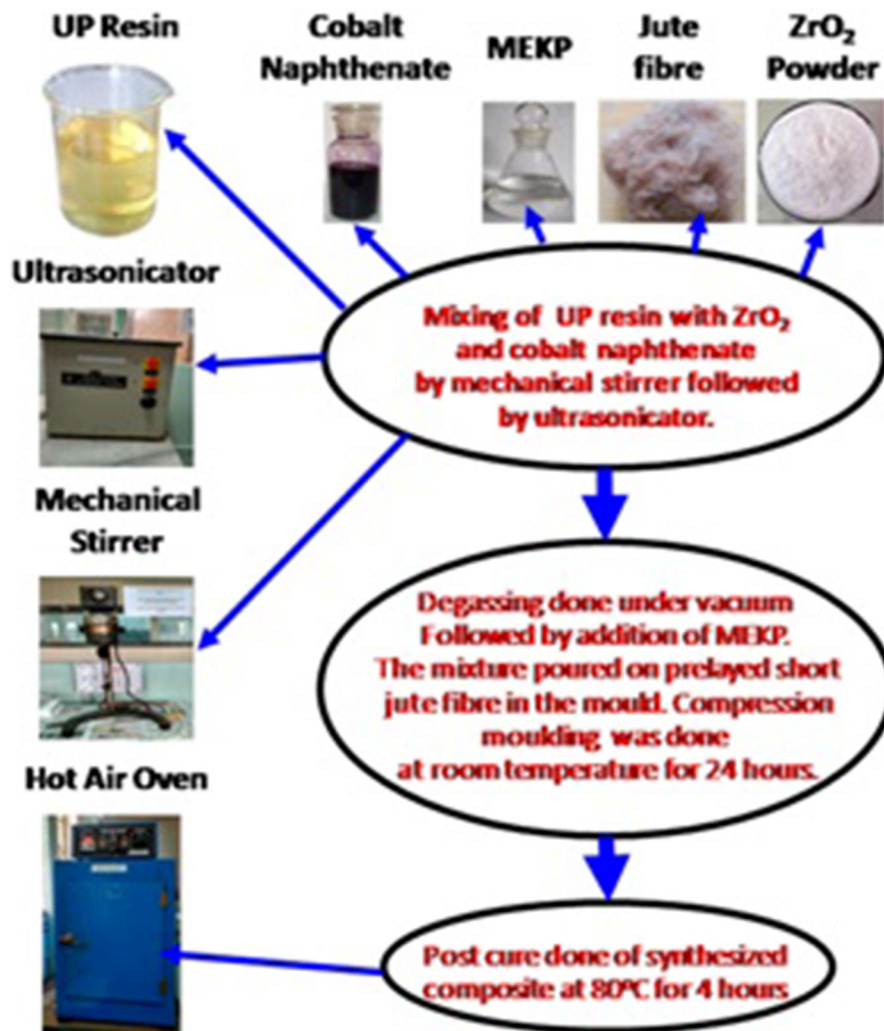
B. Biswas · P. Saha · B. C. Mitra ·  
N. R. Bandyopadhyay · A. Sinha (✉)  
Dr. M.N. Dastur School of Materials Science and  
Engineering, Indian Institute of Engineering Science and  
Technology, Shibpur, Howrah 711103, India  
e-mail: arijit@matsc.iiests.ac.in

B. Biswas  
e-mail: bhabatosh90@gmail.com

P. Sawai  
Materials Science Centre, Indian Institute of Technology,  
Kharagpur 721302, India

A. Santra · A. Gain  
Department of Industrial Chemistry and Applied  
Chemistry, Swami Vivekananda Research Center,  
Ramakrishna Mission Vidyamandira, Belur Math,  
Howrah 711202, India

## Graphical abstract



**Keywords** Natural fibre · Hybrid composite · Thermal stability · Swelling · Degradation · Failure

## Introduction

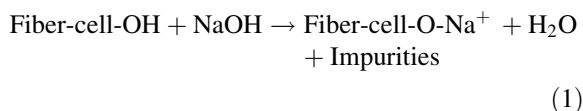
There is a substantial demand for new polymer composites incorporating natural fibers in today's research. Thermosetting polymers are generally brittle and their properties can be improved by incorporation of fibre and particulates, individually or by suitable combination of both. In either case, the physical and mechanical properties of the polymeric matrix were enhanced significantly (Van de and Kiekens

2002; Victor and Arun 2003). The untreated fibres (like jute, sisal, flax, hemp etc.) have very little adhesion with the thermosetting matrices, but the adhesion can be improved by suitable chemical treatment. This yields better bonding and considerable wetting between the fibres and matrices that improves significantly the properties and hence the performance of the fabricated composites (Narendra and Yiqi 2011; Liu et al. 2009; Mohanty et al. 2000; Satyanarayana et al. 1990). Moreover, the particles are also incompatible with the thermosetting polymer, but they can be made compatible with superior wettability by subjecting them to suitable silanization. The most essential merit of using the particulate as filler within polymeric matrix with respect to its fibre counterpart is

that a small content of the former can fetch similar or better results to that of the latter (Mohammed 2011; Kim et al. 2012; Singh et al. 2002). Another approach is to fabricate the composites by incorporation of both particle and fibre that will yield a superior resultant property than that of the individual constituent phases. This approach has been adopted by various researchers, where a small quantity of particulate has been used along with significant amount of fibrous filler which reduces the processing cost and hence yield superior properties of the composites (Sing et al. 1995). UP based, jute-reinforced, and alumina- or zirconia-filled composites possess enhanced mechanical property and better thermal stability with 20 wt% of filler content. Such types of composites display a high resistance towards chemicals and moisture absorption (Adhikari et al. 2017). Ray et al. (Ray and Eastale 2007) investigated clay based nano polymer composites that demonstrate a high barrier performance and improved thermal stability, which make these composite suitable for several applications. In this present investigation the key objective is to fabricate an economical, thermally stable and chemical resistant polymer matrix composite by dispersion of jute fibre and ZrO<sub>2</sub> particles within UP matrix.

## Materials and methods

UP resin of GP 333 grades with 35 wt% styrene, methyl ethyl ketone peroxide (MEKP) as catalyst and cobalt naphthenate as accelerator were procured from M/s A K B Agencies, 1:3, Belegkata Road, Kolkata-700015, India. UP resin is synthesized through a reaction involving C<sub>4</sub>H<sub>2</sub>O<sub>3</sub> (Methyl anhydride), C<sub>6</sub>H<sub>4</sub>(CO)<sub>2</sub>O (Phthalic anhydride) and C<sub>3</sub>H<sub>8</sub>O<sub>2</sub> (Propylene Glycol). The molecular weight, viscosity and density of the UP resin are estimated around 2800 g/mol, 600 cps and 1.12 g/cm<sup>3</sup>, respectively. The molecular weight and density of MEKP and Cobalt naphthalate are around 210.22 g/mol and 1.15 g/cm<sup>3</sup> for the former and 401.02 g/mol and 0.96 g/cm<sup>3</sup> for the latter, respectively. The procured discontinuous jute fibre (~ 3 cm) with density ~ 1.5 g/cm<sup>3</sup> and tensile strength ~ 360 MPa was treated with 5 wt% of NaOH solution for 2 h as per the following reaction (Ray et al. 2007).



The ZrO<sub>2</sub> particles (size ~ 50–70 μm; 97% Extra Pure; Loba Chemie) with density ~ 5.85 g/cm<sup>3</sup> and molecular weight ~ 123.22 g/mol were chemically modified with 1.0 wt% of silane (vinyl methoxyethylsilane) in a water and methanol solution for 5 min. During the silanization process the silane is placed on the surface of the ZrO<sub>2</sub> particles followed by drying of the wet powder at 93 °C for 30 min that yields the condensation of silanol to siloxanes (Tanoglu et al. 1998). The schematic sequence (Fig. 1) of the silanization for the ZrO<sub>2</sub> particles is depicts in the chemical reaction furnished below.

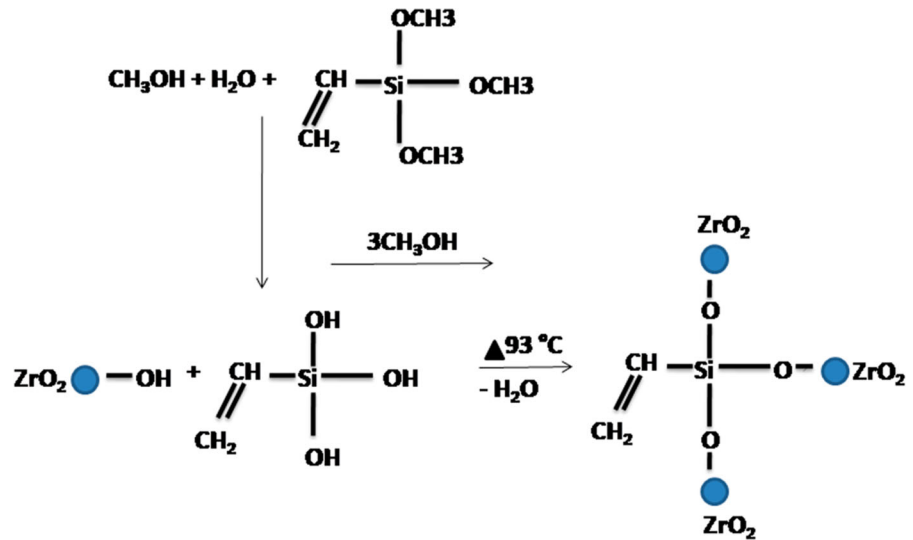
## Processing of the composites

Compression moulding technique was used for the fabrication of UP based composites with a filler (jute fibre and ZrO<sub>2</sub> particle) loading of 5, 15, 25, 35 and 45 wt%, respectively. The quantity of the ZrO<sub>2</sub> particle was selected as 10 wt% of the total filler content incorporated within the UP matrix. Initially, waxpol was applied on the inner surface of the mould for ease released of the fabricated composites followed by pre-laying of the fibre in the mould. The silanized ZrO<sub>2</sub> particle was mixed with the UP resin by mechanical stirring process. The mixture was degassed in vacuum followed by addition of accelerator and catalyst within the particle-resin mixture. The resultant mixture was then poured on the pre-layed fibre and subsequently a uniform pressure (1 kgf) was applied on the mould followed by room temperature curing for 24 h. Finally, the composite was released from the mould and subjected to post curing at 80 °C for 4 h.

## Characterization of the composites

The morphological features and degraded surface of the composites were examined by scanning electron microscope (Hitachi S-3400N) with an accelerating voltage of 15 kV. Elemental mappings of the composite was analyzed using INCA software associated with energy dispersive X-ray spectroscope (Horiba EX-250) attached with the SEM facility. The transmission electron microscopy (TEM) of the

**Fig. 1** Schematic sequence of the silanization for the  $ZrO_2$  particles



cellulosic jute fibre was conducted using Jeol JEM-2100F HRTEM at an accelerating voltage of 200 kV to investigate its morphological features and to analyze the selected area electron diffraction (SAED) pattern of the lattice fringes. The specimen for the HRTEM investigation was prepared by drop casting technique.

Fourier transform infrared spectroscopy (Bruker Tensor 27) with resolution of  $1\text{ cm}^{-1}$ , a DTGS detector, mid-IR source ( $4000$  to  $400\text{ cm}^{-1}$ ) and a KBr beam splitter was used. The thermal insulation property measurement was performed with electronic thermal insulation tester following the ASTM D1518-14 standard as per the Kawabata method (Hossen et al. 2010). The thermal stability and degradation of the composites were studied by using Thermogravimetric analyzer (NETZSCH instrument TG 209 f1; Germany) from  $30$  to  $600\text{ }^\circ\text{C}$  with a heating rate of  $10\text{ }^\circ\text{C}/\text{min}$  in  $N_2$  atmosphere. The differential thermogravimetric data was obtained from the TGA by using the software embedded within the instruments. Differential Scanning Calorimetric (DSC) analysis of the composites has been done by NETZSCH instrument. DSC analysis in  $N_2$  atmosphere was done from  $30$  to  $300\text{ }^\circ\text{C}$  with heating rate maintained as  $10\text{ }^\circ\text{C}/\text{min}$ . Flow rate of Nitrogen maintained as  $60\text{ ml}/\text{min}$ . Limiting oxygen index (LOI) measurement was done according to ASTM standard D-2863. The minimum oxygen required for ignition of the composites is termed as LOI (%). The swelling behaviour of the fabricated composites was studied in various medium

viz, neutral ( $\text{pH} \sim 7$ ), alkaline ( $\text{pH} \sim 12$ ), acidic ( $\text{pH} \sim 2$ ) and simulated sea water ( $\text{pH} \sim 7.15$ ). A high precision balance with accuracy close to  $10^{-5}\text{ g}$  was used for measurements of the swelling (wt%) of the composites. The composites were regularly weighed after an interval of 24, 48, 72, 96, 120, 144, 168, 192, 216 and 240 h, respectively for all composites in different medium with varying pH values. In this context it is worthwhile to mention that for swelling in boiling water only, the samples were weighed at 60, 120, 180, 240, 300, 360, 420, 480, 540 and 600 min, respectively. The amount of swelling was calculated at above mentioned time intervals as per the relationship (Deo and Acharya 2008).

$$W(\%) = \frac{(W_t - W_o) \times 100}{W_o} \quad (2)$$

where,  $W_t$  is the weight of the sample after swelling as a time interval of  $t$  and  $W_o$  is the weight of the sample before swelling.

## Results and discussions

### Thermal insulation measurements

Figure 2 shows the variation in thermal insulation values of different UP based composites with various filler loading. The thermal insulation increases with addition of fillers for different composites. The peak value was observed with 35 wt% of filler contents for

all types of composite. The increases in thermal insulation is monotonically from 5 wt% filler content to 35 wt% without any significant enhancement at 45 wt% of filler content. The increment in thermal insulation values up to 35 wt% of filler contents mainly due to the uniform dispersion of the insulating dispersing phase's viz, jute fibre and  $ZrO_2$  within UP matrix. Another probable reason for the enhancement may be the increase in interfacial resistant with higher fillers addition (Han 2006; Lu et al. 2005). The hollow structure of natural jute fibre (lumen) and the presence of voids within UP matrix and interface between the matrix and fillers were also responsible for the augmentation of the thermal insulation values for composites as reported elsewhere (Biswas et al. 2016, 2018; Mitra et al. 1998; Dash et al. 2000; Padal et al. 2014; Mohanty et al. 2004; Ray et al. 2002). Beyond 35 wt% saturation was observed which may be due to non-uniform or irregular dispersion of fillers with 45 wt% filler content. It was clearly revealed from the thermal insulation measurements that the 35 wt% of filler content composites displays the peak value and hence the subsequent structural, thermal as well as the swelling behaviour were performed for the said composites.

### Structural investigations

#### SEM images

The SEM images of jute fibre without and with 5% alkali treatment are shown in Fig. 3 a, b. It can be

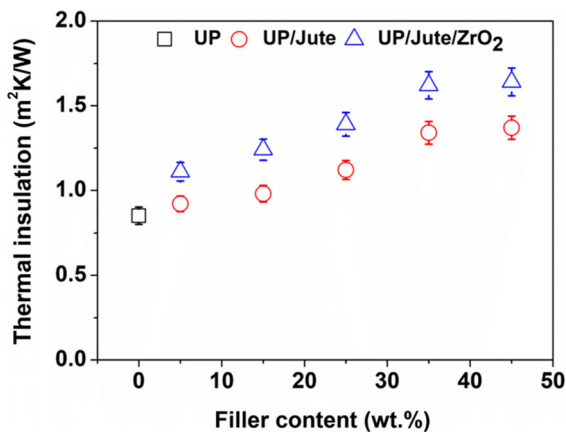


**Fig. 2** Variation of thermal insulation with fillers (wt%) addition for UP and UP based composites

visualize from the images that the rough portion of the fibre, i.e. basically the lignocelluloses has been removed from its surface. This makes the fibre more water resistant, thereby significantly improving its adhesion with the UP matrix. The SEM images of 35 wt% UP/Jute and UP/Jute/ $ZrO_2$  has been presented in Fig. 3 c, d. The uniform and consistent dispersion of the fillers i.e., fibres and  $ZrO_2$  particles (marked with white circles) within the UP matrix is quite evident from the images.

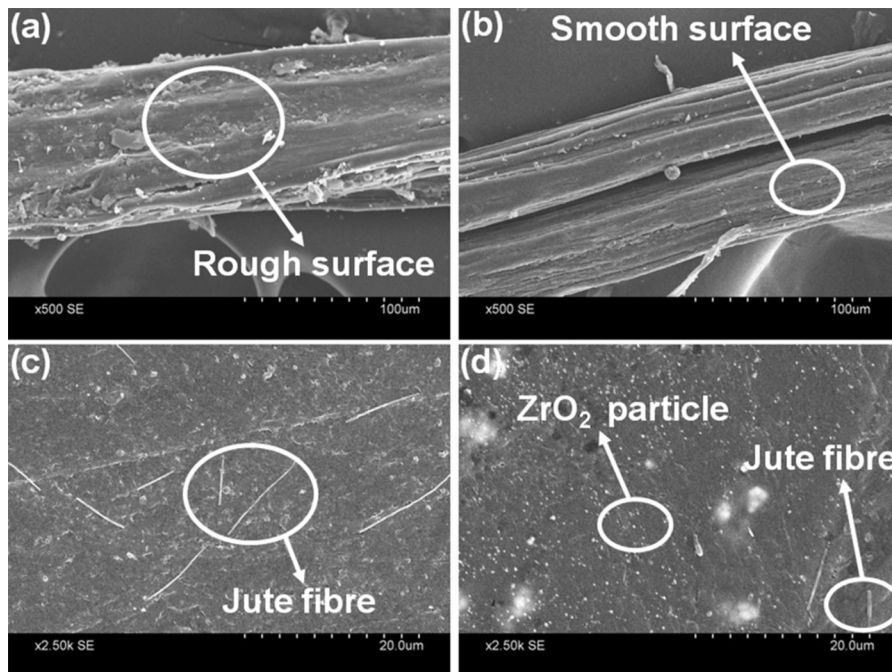
#### HR-TEM analysis

Figure 4 shows the TEM micrographs, lattice fringes and SAED pattern of cellulosic jute fibre. Figure 4 a is the alkali treated single jute fibre at low magnification showing the arrangement of fibrils at different orientations. Figure 4 b presented enlarge view of the encircled portion (Fig. 4 a) of the jute fibre that revealed a clear and distinct arrangement of the fibrils within the same due to its treatment with alkali. The shiny and clear nature was mainly due to the alkali treatment that removed the amorphous lignin and hemicelluloses from the fibre surface. Figure 4 c shows the lattice fringes in the crystalline region of the cellulosic jute fibre and the corresponding SAED pattern as inset validate the same findings. Figure 5 shows the quantitative elemental analysis of the UP/Jute/ $ZrO_2$  composites with 35 wt% filler content. The elemental mapping of the composite corroborates the presence of carbon, oxygen, zirconium, cobalt, sodium and silicon, respectively that signifies the substantial existence of the fillers (jute and  $ZrO_2$ ) within the UP matrix.

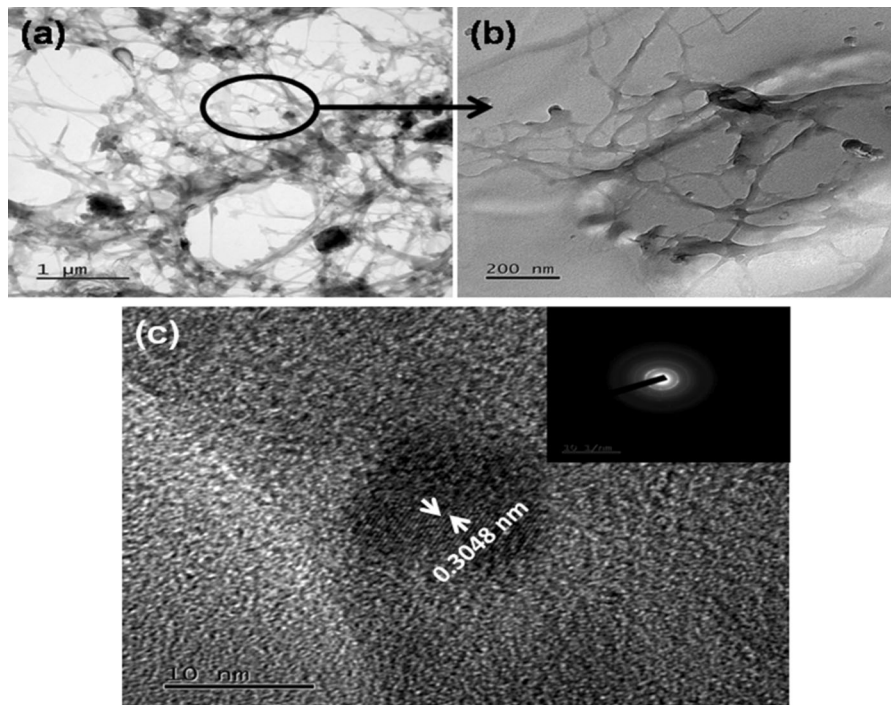
#### FT-IR analysis

Figure 6 a–d shows the FTIR patterns for UP, alkali treated jute, vinyl silane treated  $ZrO_2$  and 35 wt% UP/Jute/ $ZrO_2$ , respectively. The interaction between chemically treated fillers and UP matrix may be physical, mechanical and/or chemical (Sichina 2000). The detailed analyses of the FTIR spectra allow to draw the various interpretations. The peaks at around  $3944.19$  and  $2364.58$   $cm^{-1}$  (Fig. 6 d) are of treated jute fibres which shifted from their original positions ( $3934.55$  and  $2362.65$   $cm^{-1}$  in Fig. 6 b) due to its in plane displacement. The peaks at around  $3438.87$  and  $3859.33$   $cm^{-1}$  (Fig. 6 d) are due to intermolecular





**Fig. 3** SEM images of **a** untreated jute, **b** 5% alkali treated jute, **c** UP/Jute and **d** UP/Jute/ZrO<sub>2</sub> composites with 35 wt% filler content



**Fig. 4** HRTEM images of **a** 5% alkali treated jute fibre, **b** enlarge view of the encircled portion of the fibre and **c** lattice fringes in the crystalline region of the fibre with SAED pattern of the same as inset

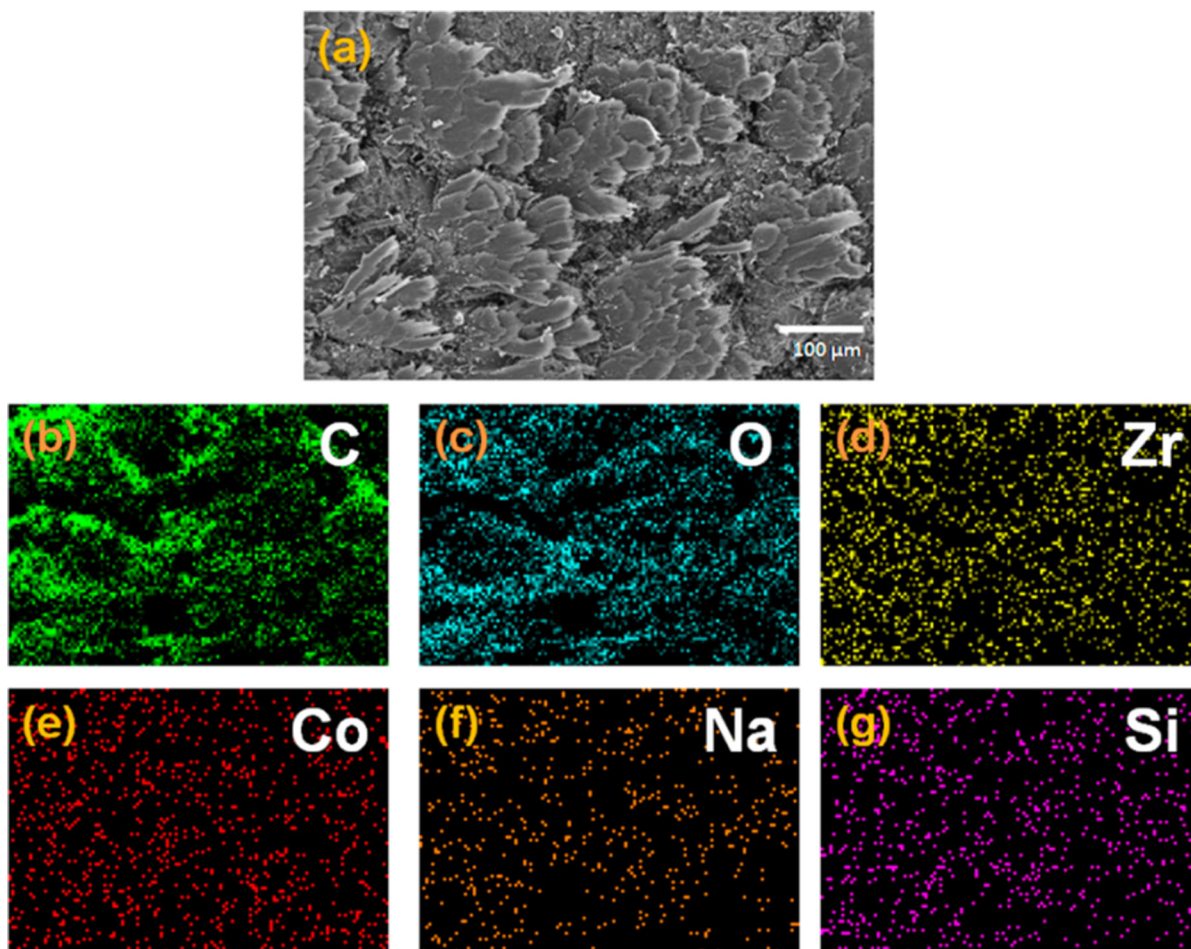


**Fig. 5** Elemental mappings of the **a** UP/Jute/ZrO<sub>2</sub> composites with 35 wt% filler content corroborating the presence of **b** carbon, **c** oxygen, **d** zirconium, **e** cobalt, **f** sodium and **g** silicon, respectively

hydrogen bonding arises from the interaction between the carboxylic group (–COOH) of anhydride and the hydroxyl groups (–OH) of the UP. The 3770.61 cm<sup>-1</sup> (Fig. 6d) peak is of UP matrix which shifted from 3776.39 cm<sup>-1</sup> (Fig. 6a) due to layer symmetric stretching vibration of aliphatic hydrocarbon C–H group. The two new peaks appeared at 3068 and 3026.13 cm<sup>-1</sup> (Fig. 6d) are mainly due to isometric stretching of –CH<sub>2</sub> group at the matrix-filler interface between filler and matrix (Bar et al. 2015). The peak observed at 1730.04 cm<sup>-1</sup> (Fig. 6d) is due to the strong carbonyl stretching of UP matrix. The peaks at 1957.63 and 1593.10 cm<sup>-1</sup> (Fig. 6d) of UP matrix are shifted from 1959.56 to 1591.17 cm<sup>-1</sup> (Fig. 6a) due to the stretching vibration of phenyl group. The peaks at 746.40 and 543.89 cm<sup>-1</sup> (Fig. 6d) of UP matrix are shifted from 742.55 to 536.17 cm<sup>-1</sup> (Fig. 6a) due to

the matrix-filler interactions (Sichina 2000); (Han and Fina 2011)]. The peak at 1379.02 cm<sup>-1</sup> (Fig. 6d) for UP matrix arises mainly due to layer symmetric stretching vibration of aliphatic hydrocarbon C–H group. The peaks at 1278.72, 1068.50 and 1132.14 cm<sup>-1</sup> (Fig. 6d) are due to ZrO<sub>2</sub> particle which shifted from their original positions at 1277, 1064 and 1132 cm<sup>-1</sup> (Fig. 6c) as a results of chemical and mechanical interaction between matrix and fillers (Idicula et al. 2006).

#### Thermal properties measurements

##### *Thermogravimetric analysis (TGA)*

Figure 7 shows the TGA plots for UP matrix as well as UP based composites depicting the thermal stability

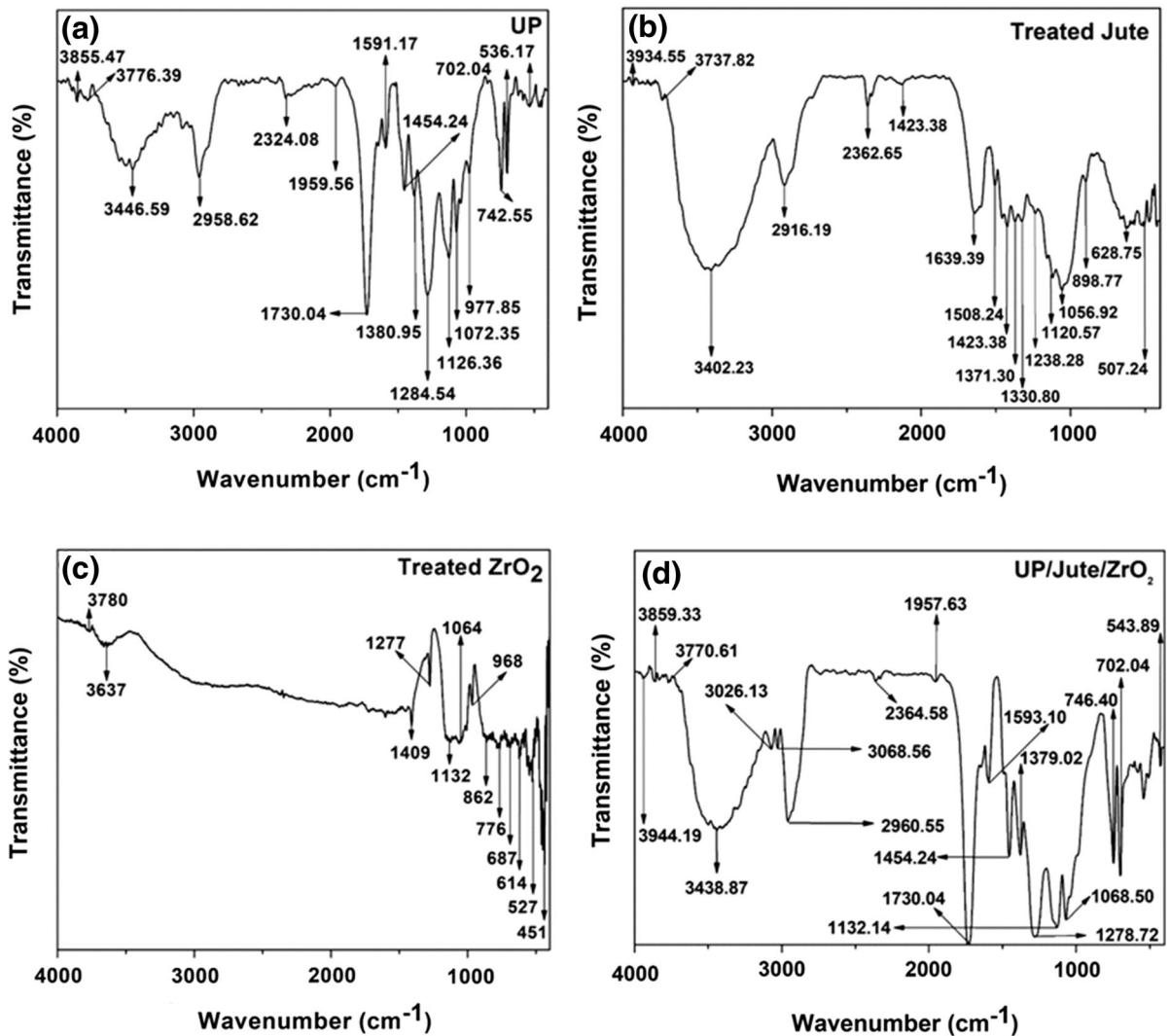


**Fig. 6** FT-IR spectra for **a** UP, **b** treated jute, **c** treated  $\text{ZrO}_2$  and **d** 35 wt% UP/Jute/ $\text{ZrO}_2$

and weight loss during thermal activation. The plots further corroborated the fact that the thermal stability of UP and UP based composites are in the range of 38–80 °C. The thermal stability temperature and corresponding residual weight (%) at 600 °C are illustrated in Table 1. It is clearly revealed that the thermal stability temperature ( $\sim 80.27$  °C) is highest for UP/Jute/ $\text{ZrO}_2$  as compared to UP matrix ( $\sim 38.12$  °C) and UP/Jute composites ( $\sim 68.80$  °C), respectively. This may be due to the better dispersion of the fillers (jute and  $\text{ZrO}_2$ ) within the UP matrix. In the case of UP/Jute composites, the uniform dispersion of jute within UP matrix is limited due to fibrous form of the former. As a result, for this type of composites,

the stability of the polymeric matrix under thermal activation is lower than UP/Jute/ $\text{ZrO}_2$  composites. The UP/Jute/ $\text{ZrO}_2$  composites display an enhanced stability under thermal activation as compared to UP/Jute composites due to better dispersion and non-degradability of the  $\text{ZrO}_2$  particulate within UP matrix whereas in case of latter both matrix and jute are susceptible to degradation under the same condition. This also substantiates the fact that the residual weight at maximum temperature ( $\sim 600$  °C) is more for UP/Jute/ $\text{ZrO}_2$  ( $\sim 3.725\%$ ) as compared to UP/Jute composites ( $\sim 2.125\%$ ) and the UP matrix ( $\sim 1.315\%$ ) (Adhikari et al. 2017; Victor and Arun 2003; Narendra and Yiqi 2011).



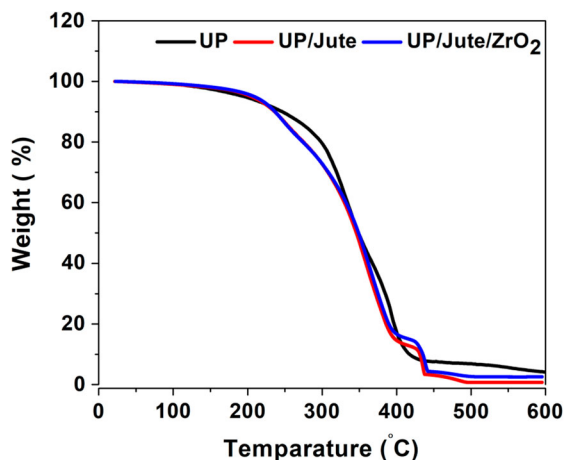


**Fig. 7** TGA plots for UP, UP/Jute and UP/Jute/ZrO<sub>2</sub> composites

#### Differential thermogravimetric analysis (DTGA)

Figure 8 a–c shows the DTGA plots (obtained by differentiating the TGA plots) of UP and UP based composites which demonstrates the degradation temperature of the matrix as well as the composites. The DTGA plots revealed various associated events viz, pre-degradation and degradation during heating of the samples. The value of pre-degradation and degradation temperature are appended in Table 1. The DTGA plots show a maximum degradation temperature for UP/Jute/ZrO<sub>2</sub> as compared to UP/Jute composites and UP matrix. This may be due to uniform dispersion of the ZrO<sub>2</sub> particle and better bonding of the fillers (jute and ZrO<sub>2</sub> particle) within the UP matrix. Moreover, higher energy is utilized in breaking the bonds between UP matrix and fillers (jute and ZrO<sub>2</sub>) in the case of UP/Jute/ZrO<sub>2</sub> composites than UP/Jute composites (Narendra and Yiqi 2011; Idicula et al. 2006; Takagi et al. 2007). The degradation results in complete breakdown of both weak and strong bonds within matrix and fillers as well as between the same.

**Table 1** Thermal behaviour of UP and UP based composites

Samples	Thermal stability (°C)	Pre-degradation temperature (°C)	Degradation temperature (°C)	Residual weight at 600 °C (%)
UP	38.12	335.62	393.12	1.315
35 wt% UP/Jute	68.80	360.11	434.02	2.125
35 wt% UP/Jute/ZrO <sub>2</sub>	80.27	364.60	437.43	3.725

In this context it is worthwhile to mention that the pre-degradation event may occur probably due to the breakage of C–C as well as C–H bonds in case of the UP matrix and for the cellulosic fibre (jute). It is quite interesting to note that a completely new peak (encircled) was evolved in the case of UP/Jute (~ 246.18 °C) and UP/Jute/ZrO<sub>2</sub> (~ 247 °C) composites mainly due to breakage of weak Van der Waals and OH bonds in UP and jute fibre as well as the hydrogen bonds between UP matrix and fillers.

#### Differential thermal analysis (DTA)

The DTA plots of UP, UP/Jute and UP/Jute/ZrO<sub>2</sub> composites are shown in Fig. 9. It is clearly observed from the plots that a mild endothermic reaction was occurred in the temperature range of 36–65 °C and high endothermic reaction take place at a temperature above 400 °C for UP, UP/Jute and UP/Jute/ZrO<sub>2</sub> composites. It also observed that the reaction shifted towards right for UP/Jute and UP/Jute/ZrO<sub>2</sub> composites than for the UP matrix. The initial peaks may reflect the glass transition temperature ( $T_g$ ) and the higher value is for thermal degradation of the matrix and its composites, respectively. This confirmed the fact that with addition of fillers, an enhancement in thermal stability takes place.

#### DSC measurements

DSC measurement was performed on the UP and UP based composites (Fig. 10) in order to visualize the effect of fillers on  $T_g$ . The broad endothermic peaks were observed due to the presence of absorbed water in the jute fibre. A very little broadening of endothermic peak was observed in this region below 100 °C. Hence it can be concluded that the fabricated composites possess a very negligible amount of moisture (Behzad and Sain 2007).

**Fig. 8** DTGA plots for **a** UP, **b** UP/Jute and **c** UP/Jute/ZrO<sub>2</sub> composites

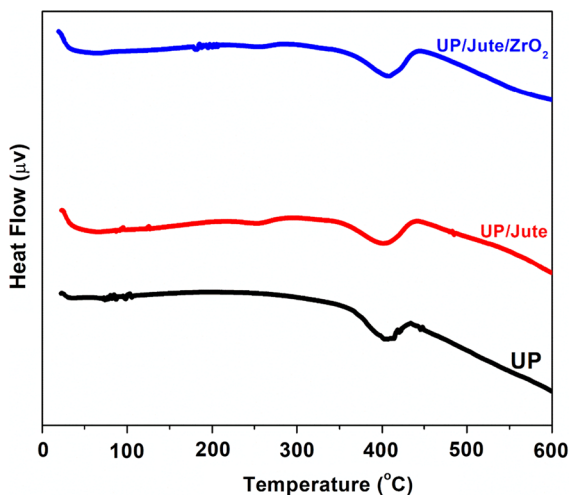
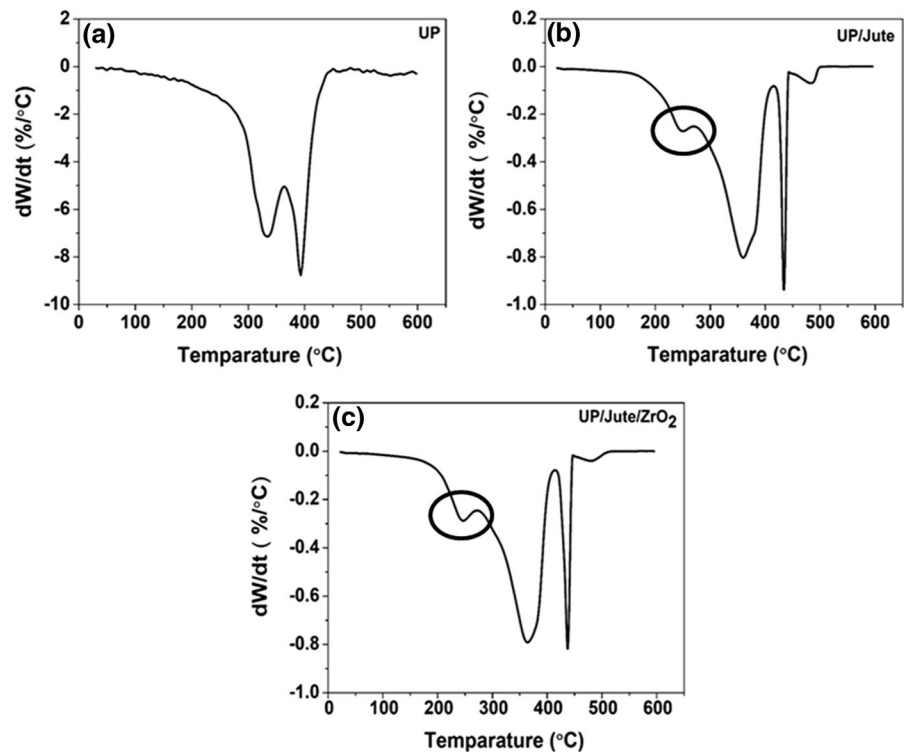


**Fig. 9** DTA plots of UP and UP based fibre reinforced composites with 35 wt% filler content

Several studies established that the enthalpy change in this region was much higher than that expected from the mere contribution of the moisture. Hence, the peak in this region was related to the  $T_g$  (Al-Nassar 2006) i.e., for UP ( $\sim 40^\circ\text{C}$ ), UP/Jute ( $\sim 65^\circ\text{C}$ ) and UP/Jute/ZrO<sub>2</sub> ( $\sim 85^\circ\text{C}$ ), respectively. A significant

increase in  $T_g$  was observed for the UP/Jute/ZrO<sub>2</sub> composite than UP/Jute composites. This may be due to the proper distribution of the fillers within the UP matrix (Zou et al. 2003; Ning and Chou 1995; Verma et al. 1991; Mounika et al. 2012).

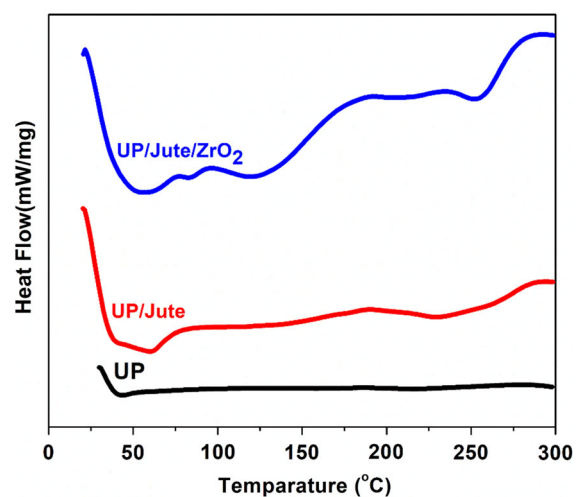


**Fig. 10** DSC plots of UP and UP based composites with 35 wt% filler content

### Limiting oxygen index (LOI) measurements

The Limiting oxygen index (LOI) measurements as per the ASTM D-2863 standard were used in the present investigation (Fig. 11) to indicate the relative flammability of UP and UP based composites. The value of the LOI signifies the minimum percentage of oxygen [O<sub>2</sub>] in the oxygen/nitrogen mixture (O<sub>2</sub>/N<sub>2</sub>) and expressed as:

$$\text{LOI} = 100 \times [\text{O}_2 / (\text{O}_2 + \text{N}_2)] \quad (3)$$

The higher the LOI value, the better is the flame retardant property of the composites (Fenimore and Martin 1999; Camino et al. 1988; Laoutid et al. 2009).

It is clearly observed from Table 2, that the UP/Jute/ZrO<sub>2</sub> composites have best LOI value of 25%. Thus, ZrO<sub>2</sub> addition in the UP/Jute not only increases the thermal stability but also enhanced the fire retardant properties. In composites char formation occurred [Fig. 11b, d and f] which was the most vital cause for the improvement of flame retardancy as these char provide a physical mask of oxygen and heat around the unburnt portion of the composites that results in the enhancement of the LOI values (Knuutinen and Kyllonen 2006). Figure 11 shows the SEM micrographs of UP [Fig. 11 a, b], UP/Jute [Fig. 11 c, d] and UP/Jute/ZrO<sub>2</sub> composite [Fig. 11 e, f] subjected to LOI measurements. The images revealed a clear formation of char in the case of UP and UP based composites. In this context, it is worthwhile to mentioned that severe air trapped zones were observed

in the case of UP matrix (Fig. 11 b), whereas this tendency was minimal for the composites with better char formation in the case with UP/Jute/ZrO<sub>2</sub> composite. [Figure 11 g–i] presented the photographic images of the UP, UP/Jute and UP/Jute/ZrO<sub>2</sub> composites after LOI testing.

### Swelling behaviour

#### Room temperature condition

Figure 12 a shows the swelling tendency of UP, UP/Jute and UP/Jute/ZrO<sub>2</sub> composites carried out at the room temperature condition with pH ~ 7. The swelling was measured at various time intervals viz. 24, 48, 72, 96, 120, 144, 168, 192, 216 and 240 h, respectively. It was clearly visualized that with passage of time, the swelling tendency was quite higher for composites as compare to the UP matrix. The swelling mainly take place through the macro and micro-voids, pores, cracks and the interfacial gap between matrix and fillers (Deo and Acharya 2008). In the case of UP/Jute composite, the tendency of swelling was severe as jute fibres tend to absorb higher amount of moisture whereas this propensity was lesser for UP/Jute/ZrO<sub>2</sub> composite due to the hydrophobicity of ZrO<sub>2</sub> particulate and its uniform dispersion within the UP matrix (Dhakal et al. 2007).

Figure 12 b shows the variation of microhardness subsequent to swelling at the room temperature

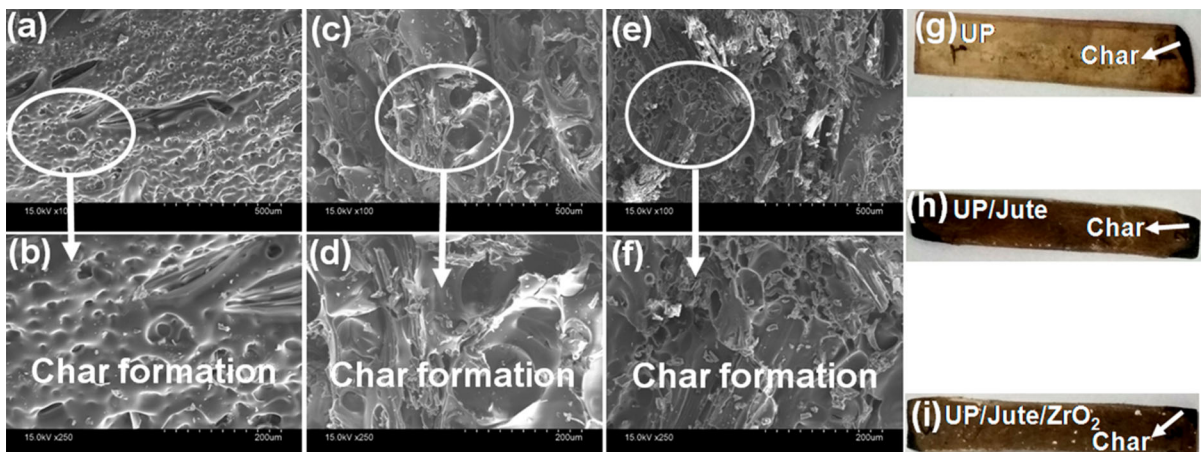


**Fig. 11** a–f SEM micrographs of UP and UP based composites subjected to LOI testing and g–i photographic images of UP and UP based composites post LOI test

**Table 2** LOI values of UP and UP based composites with 35 wt% filler content

Samples	LOI value (%)
UP	20
UP/Jute	23
UP/Jute/ZrO <sub>2</sub>	25

condition. A significant microhardness reduction was observed for UP and.

UP based composites with the worst result observed for UP/Jute composites (~ 30% reduction) as jute fibres tend to absorb more moisture which drastically affects its surface property. On the contrary, a better result was obtained for UP/Jute/ZrO<sub>2</sub> (~ 23% reduction only) due to uniform dispersion of the hydrophobic ZrO<sub>2</sub> particulate within the UP matrix.

Figure 12 c, d presented the SEM micrographs of the swelled surfaces for 35 wt% UP/Jute/ZrO<sub>2</sub> composite. It was observed that the swelling at the room temperature condition deteriorate the surface significantly. The matrix degrades drastically without any signature of fibre protruding from its surface, which is an indication of better interfacial bonding and hence

superior stability of the fabricated composites in the room temperature swelling condition.

### Boiling water condition

Figure 13 a shows the swelling behaviour of UP, UP/Jute and UP/Jute/ZrO<sub>2</sub> composites carried out at boiling water condition. The swelling was estimated at various time intervals viz. 60, 120, 180, 240, 300, 360, 420, 480, 540 and 600 min, respectively. In this case, the swelling behaviour of UP and UP based composites was rapid as compare to the room temperature swelling. It was clearly visualized from the Fig. 13 a that with course of time, the swelling tendency was higher for UP based composites as compare to the UP matrix. In this condition the swelling mostly occurred through the voids, pores, cracks present on and below the surface of the composites as well as within the interfacial gap between matrix and fillers.

Figure 13 b revealed the variation of microhardness after swelling at the boiling water condition. A significant reduction in microhardness values was observed in this case when compared to the samples swelled at room temperature condition. The worst result noticed for UP/Jute composites (~ 43%

**Fig. 12** a Room temperature swelling behaviour of UP, UP/Jute and UP/Jute/ZrO<sub>2</sub> composites, b effect of swelling on the microhardness and c, d SEM micrographs of water swelled surface for 35 wt% UP/Jute/ZrO<sub>2</sub> composite

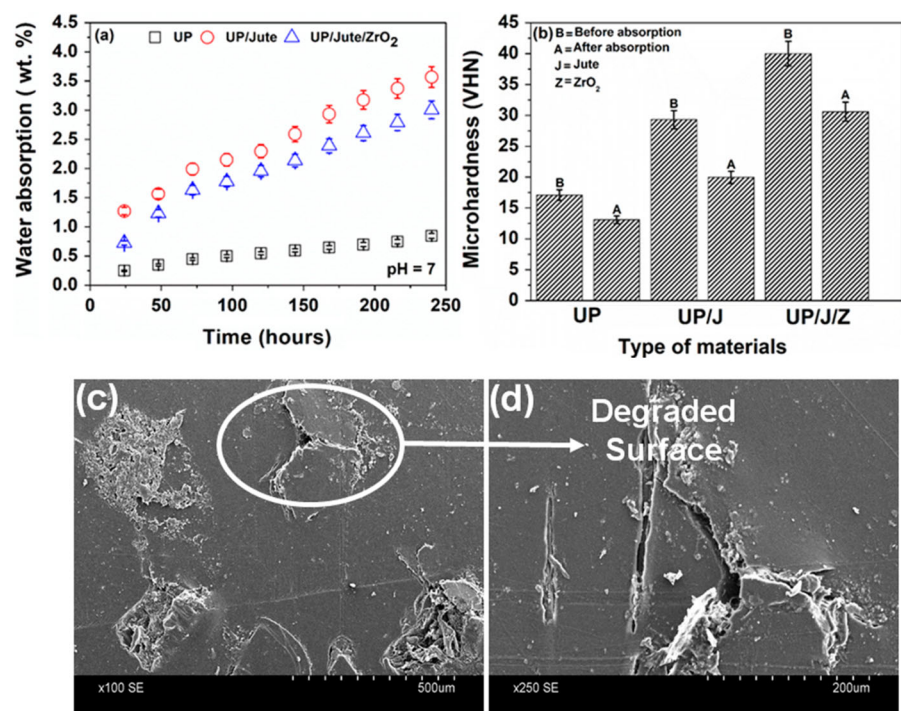
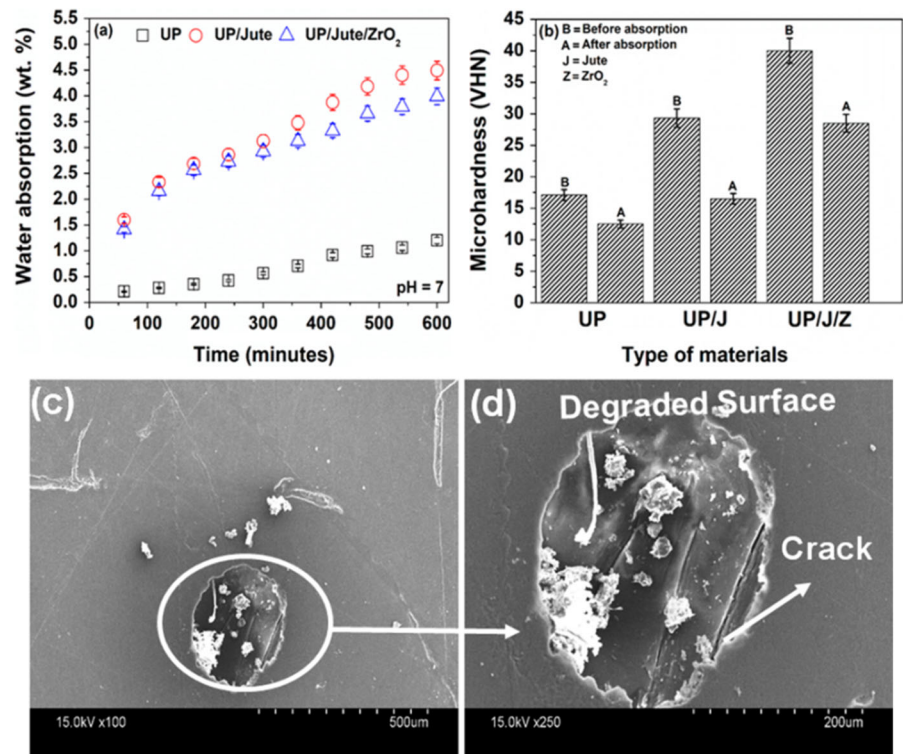




**Fig. 13** **a** Swelling behaviour at boiling water for UP, UP/Jute and UP/Jute/ZrO<sub>2</sub> composites, **b** effect of swelling on the microhardness and **c, d** SEM micrographs of swelled surface for 35 wt% UP/Jute/ZrO<sub>2</sub> composite



reduction) as in boiling water the jute fibre absorbed more moisture thereby affecting its surface drastically. Moreover, the better result obtained for UP/Jute/ZrO<sub>2</sub> (~ 28% reduction), as the hydrophobic ZrO<sub>2</sub> particulate were well dispersed within the UP matrix.

The SEM micrographs as presented in Fig. 13 c, d shows the surface of 35 wt% UP/Jute/ZrO<sub>2</sub> composite after swelling in boiling water. It was observed that the swelling at the boiling water leads to severe degradation of the surface when compared to the room temperature condition. The matrix degrades severely with a tendency of fibre protruding as well as cracks generation on its surface. This justify the facts that the degradation occurred in boiling water is more drastic than room temperature condition.

#### Alkaline water condition

The swelling tendency of UP, UP/Jute and UP/Jute/ZrO<sub>2</sub> composites carried out at the alkaline water condition with pH~ 12 as shown in Fig. 14 a. The swelling was evaluated at various time intervals viz. 24, 48, 72, 96, 120, 144, 168, 192, 216, 240 h, respectively. Like previous two conditions, it was

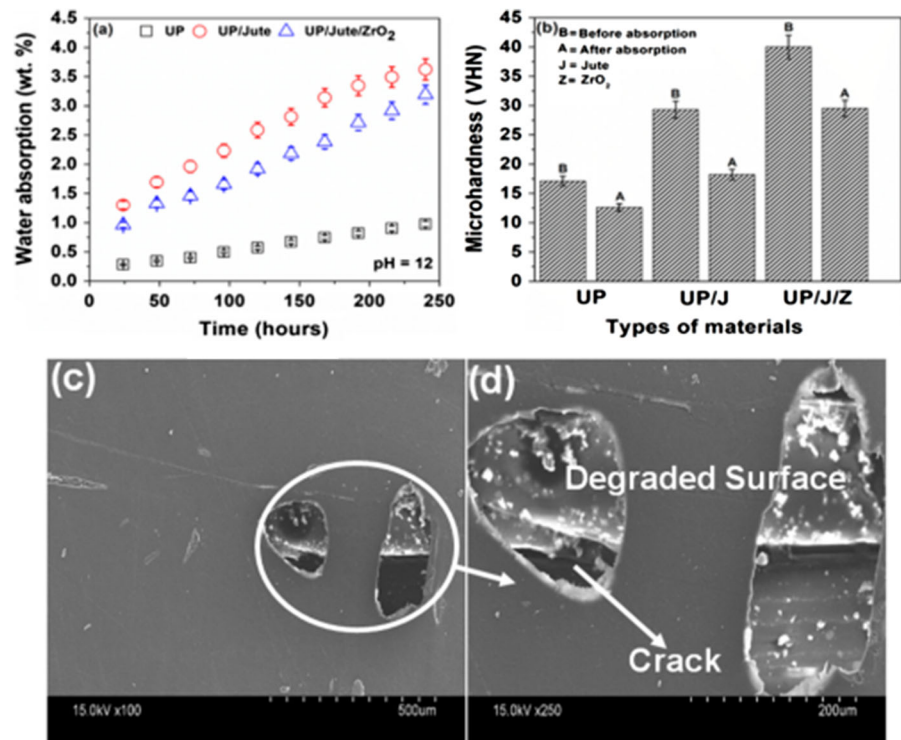
clearly visualized that with passage of time, the swelling tendency was quite higher for composites as compare to the UP matrix. The swelling mainly take place through various defects like voids, cracks, pores, as well as within the interfacial gap between matrix and fillers. For UP/Jute composite, the swelling tendency was extreme as jute fibres tend to attract higher amount of moisture while such tendency was limited for UP/Jute/ZrO<sub>2</sub> composite due to the hydrophobicity of ZrO<sub>2</sub> particulate and its uniform dispersion within the UP matrix.

Figure 14 b revealed the variation of microhardness after swelling at the alkaline water condition. A significant reduction in microhardness was observed which was much higher than the room temperature condition. The post swelling microhardness reduction for UP/Jute (~ 38%) and UP/Jute/ZrO<sub>2</sub> (~ 26%) composites were more and rapid as compare to the room temperature condition as a results its affects the surface severely.

Figure 14 c, d presented the SEM micrographs showing the surfaces swelled in alkaline water for 35 wt% UP/Jute/ZrO<sub>2</sub> composite. It was revealed that the surfaces swelled in the presence of alkaline water



**Fig. 14** **a** Swelling behaviour at alkaline water condition for UP, UP/Jute and UP/Jute/ZrO<sub>2</sub> composites, **b** effect of swelling on the microhardness and **c, d** SEM micrographs of swelled surface for 35 wt% UP/Jute/ZrO<sub>2</sub> composite



degraded drastically as compare to the room temperature condition.

#### Acidic water condition

Figure 15 a revealed the swelling behaviours of UP, UP/Jute and UP/Jute/ZrO<sub>2</sub> composites which carried out at the acidic water condition with pH ~ 2. The swelling was computed at different time intervals viz. 24, 48, 72, 96, 120, 144, 168, 192, 216, 240 h, respectively. It was clearly visualized from the Fig. 15 a that with passage of time, the swelling propensity was quite higher for composites as compare to the UP matrix that take place primarily through the voids, pores, cracks and the interfacial gap between matrix and fillers. Similar to the room temperature as well as alkaline conditions, the UP/Jute composite possesses maximum swelling tendency due to higher amount of moisture absorbance by jute fibre, whereas this affinity was less for UP/Jute/ZrO<sub>2</sub> composite due to the hydrophobicity of ZrO<sub>2</sub> particulate along with its uniform dispersion within the UP matrix.

Figure 15 b revealed the post swelling variation of microhardness values submerged within the acidic water. It was clearly noticed that a noteworthy

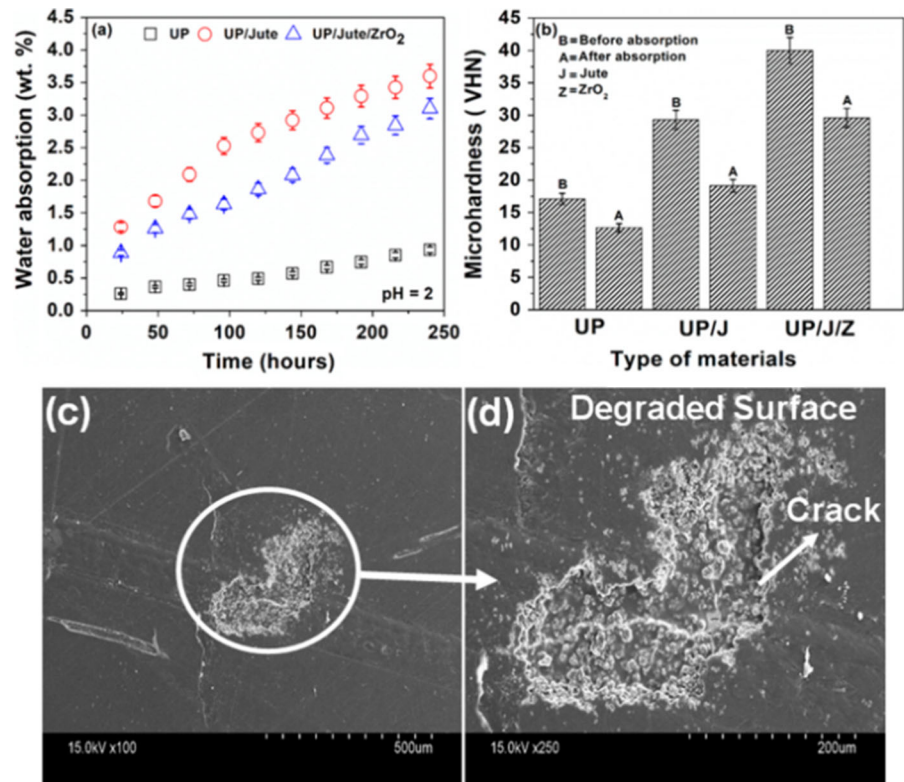
microhardness reduction occurred for UP/Jute (~ 34% reduction) and UP/Jute/ZrO<sub>2</sub> (~ 25% reduction) composites which is higher than the room temperature but lesser than the alkaline condition swelling.

Figure 15 c, d presented the SEM images of swelled surfaces for 35 wt% UP/Jute/ZrO<sub>2</sub> composite in the acidic water condition. It was observed that the surface degradation due to swelling in the acidic water was severe than the room temperature condition. The matrix degrades extensively without any signature of fibre protruding although a significant presence of cracks on the surface was inevitable which is very similar to alkaline water condition.

#### Simulated sea water condition

The sea water condition was prepared following the ASTM D-1141 standards by maintaining a composition of NaCl (24.53 g/l), MgCl<sub>2</sub> (5.20 g/l), Na<sub>2</sub>SO<sub>4</sub> (4.09 g/l), CaCl<sub>2</sub> (1.16 g/l), KCl (0.695 g/l), and NaHCO<sub>3</sub> (0.201 g/l) (Saadatmanesh et al. 2010). Figure 16 a shows the swelling behaviours of UP, UP/Jute and UP/Jute/ZrO<sub>2</sub> composites submerged in the simulated sea water with pH ~ 7.15. The swelling

**Fig. 15** **a** Swelling behaviour at acidic water for UP, UP/Jute and UP/Jute/ZrO<sub>2</sub> composites, **b** effect of swelling on the microhardness and **c, d** SEM micrographs of swelled surface for 35 wt% UP/Jute/ZrO<sub>2</sub> composite



calculated at various time intervals viz. 24, 48, 72, 96, 120, 144, 168, 192, 216, 240 h, respectively. Like all previous conditions it was clearly observed that with passage of time, the swelling that largely take place through the voids, pores, cracks and the interfacial gap was superior for composites as compare to the UP matrix. In the simulated sea water condition an identical swelling tendency was observed just like all other previous submerged cases with the maximum for UP/Jute as compared to UP/Jute/ZrO<sub>2</sub> composite as the fibres be likely to absorb more amount of moisture whereas such tendency was minimum for UP/Jute/ZrO<sub>2</sub> composite due to the hydrophobic nature of ZrO<sub>2</sub> particulate as well as its uniform dispersion within the UP matrix.

Figure 16 b shows the variation of microhardness after swelling at the simulated sea water condition. A considerable microhardness reduction was observed i.e., ~ 33% for UP/Jute and ~ 24% for UP/Jute/ZrO<sub>2</sub>, the values much higher than the room temperature but lower than the alkaline and acidic swelling condition. This substantiate the fact that the composites absorbed moisture more quickly at simulated sea

water condition than the room temperature water condition that significantly affects its surface.

Figure 16 c, d shows the SEM micrographs of swelled surfaces for 35 wt% UP/Jute/ZrO<sub>2</sub> composite subjected to the simulated sea water condition. It was clearly revealed that the swelling at the simulated sea water condition slightly deteriorate the surface with formation of few cracks in comparison with the swelled surfaces submerged in alkaline, acidic and boiling water.

## Conclusions

From the present investigation it was observed that along with fillers addition i.e., chemically treated discontinuous jute fibre and ZrO<sub>2</sub>, the thermal stability, degradation temperature and thermal insulation of the fabricated composites improved significantly. Moreover, the swelling behaviour shows a remarkable improvement with the addition of silane treated ZrO<sub>2</sub> as filler. The composites viz. UP/Jute and UP/Jute/ZrO<sub>2</sub> with 35 wt% filler content display the best results with respect to thermal stability, degradation

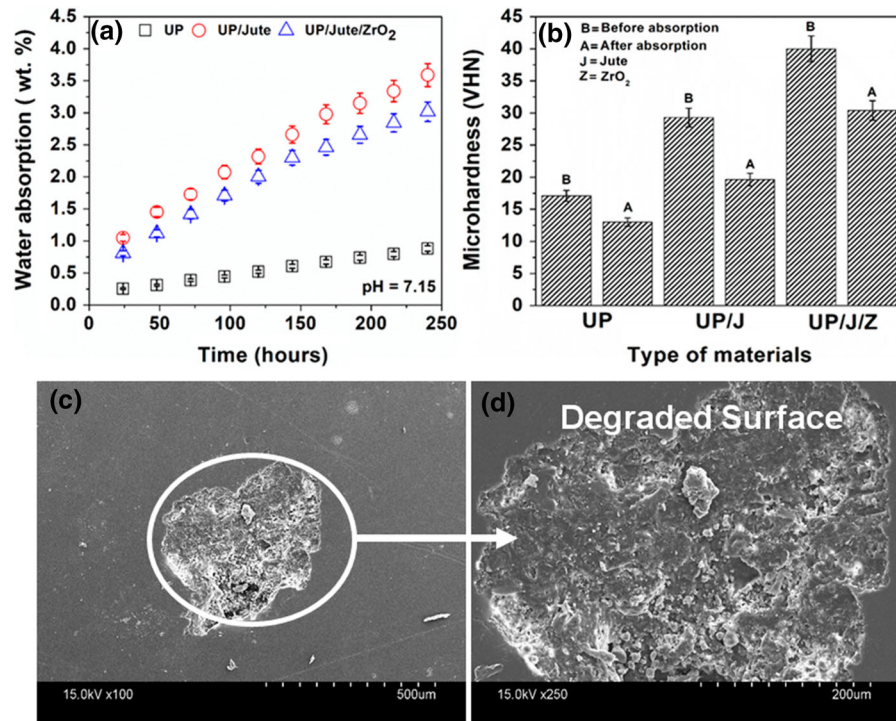


**Fig. 16** **a** Swelling behaviour at simulated sea water condition for UP, UP/Jute and UP/Jute/ZrO<sub>2</sub> composites, **b** effect of swelling on the microhardness and **c, d** SEM micrographs of swelled surface for 35 wt% UP/Jute/ZrO<sub>2</sub> composite

temperature and insulation as well as swelling behaviours. Moreover, it was further established that the UP/Jute/ZrO<sub>2</sub> composites show superior results with a significant improvement in thermal stability, thermal insulation and degradation temperature along with satisfactorily swelling behaviour after submerging in the solutions with a range of pH values.

**Acknowledgments** Author Bhabatosh Biswas is highly indebted to Indian Institute of Engineering Science and Technology (IIEST), Shibpur, India for providing the Institute fellowship to carry out his research work.

## References

- Adhikari J, Biswas B, Chabri S, Bandyopadhyay NR, Sawai P, Mitra BC, Sinha A (2017) Effect of functionalized metal oxides addition on the mechanical, thermal and swelling behavior of polyester/jute composites. *Eng Sci Technol* 20:760–774
- Al-Nassar YN (2006) Prediction of thermal conductivity of air voided-fiber-reinforced composite laminates part II: 3D simulation. *Heat Mass Transf* 43:117–122
- Bar M, Alagirusamy R, Das A (2015) Flame retardant polymer composites. *Fiber Polym* 16:705–717
- Behzad T, Sain M (2007) Measurement and prediction of thermal conductivity for hemp fiber reinforced composites. *Polym Eng Sci* 47:977–983
- Biswas B, Chabri S, Sawai P, Mitra BC, Das K, Sinha A (2016) Effect of copper incorporation on the mechanical and thermal behavior of jute fiber reinforced unsaturated polyester composites. *Polym Compos* 39:E 1315–1321
- Biswas B, Chabri S, Sawai P, Mitra BC, Das K, Sinha A (2018) Effect of aluminium addition on the mechanical and thermal behaviour of unsaturated polyester/jute composites. *J Inst Eng* 99:525–530
- Camino G, Costa L, Casorati E, Bertelli G, Locatelli R (1988) *J Appl Polym Sci* 35:1863–1867
- Dash BN, Rana AK, Mishra HK, Nayak SK, Tripathy SS (2000) Novel Low-cost jute-polyester composites. III. weathering and thermal behavior. *J Appl Polym Sci* 78:1671–1679
- Deo C, Acharya SK (2008) Preparation and properties of biodegradable poly (propylene carbonate)/thermoplastic dried starch composites. *Carbohydr Polym* 71:229–234
- Dhakal HN, Zhang ZY, Richardson MOW (2007) Effect of water absorption on the mechanical properties of hemp fibre reinforced unsaturated polyester composites. *Compos Sci Technol* 67:1674–1683
- Fenimore CP, Martin FJA (1999) Study of optimum fibre content in unit composite. *Mod Plast* 44:141–146
- Han Z (2006) Two phase studies of unsaturated polyester. 3:11–19.

- Han Z, Fina A (2011) Thermal conductivity of carbon nanotubes and their polymer nanocomposites: a review. *Prog Polym Sci* 36:914–944
- Hossen MF, Hamdan S, Rahman MR, Rahman MM, Liew FK, Lai JC (2010) Effect of moisture absorption on mechanical properties of chopped natural fiber reinforced epoxy composite. *J Reinf Plast Compos* 29:2513–2521
- Idicula M, Boudenne A, Umadevi L, Ibos L, Candau Y, Thomas S (2006) Thermo-physical. Properties of natural fibre reinforced polyester composites. *Compos Sci Technol* 66:2719–2725
- Kim HJ, Jung DH, Jung IH, Cifuentes JI, Rhee KY, Hui D (2012) Enhancement of mechanical properties of aluminium/epoxy composites with silane functionalization of aluminium powder. *Compos Part B* 43:1743–1748
- Knuutinen U, Kyllonen P (2006) *E- preserv. Sci.*, 3:11–16.
- Laoutid F, Bonnaud L, Alexandre M, Lopez-Cuesta JMR (2009) New prospects in flame retardant polymer materials: from fundamentals to nanocomposites. *Mater Sci Eng* 63:100–106
- Liu L, Iannyong YuJ, Cheng L, Qu W (2009) Mechanical properties of poly (butylene succinate) (PBS) biocomposites reinforced with surface modified jute fibre. *Compos Part A* 40:669–674
- Lu J, Wu Z, Negulescu V (2005) Wood-fiber/high-density-polyethylene composites: coupling agent performance. *J Appl Polym Sci* 96:93–102
- Mitra BC, Basak RK, Sarkar M (1998) Studies on jute-reinforced composites Its limitations, and some solutions through chemical modifications of fibers. *J Appl Polym Sci* 67:1093–1100
- Mohammed MA (2011) Mechanical behavior for polymer matrix composite reinforced by copper powder. *Coll Eng J (NUCEJ)* 14:160–176
- Mohanty AK, Misra M, Hinrichsen G (2000) Biofibres, biodegradable polymers and biocomposites: an overview. *Macromol Mat Eng* 276–277:1–24
- Mohanty S, Nayak SK, Verma SK, Tripathy SS (2004) Effect of MAPP as a coupling agent on the performance of jute–pp composites. *J Reinf Plast Compos* 23:625–637
- Mounika M, Ramaniah K, Prasad AVR, Rao KM, Reddy KHC (2012) Thermal conductivity characterization of bamboo fiber reinforced polyster composite. *J Mater Environ Sci* 3:1109–1116
- Narendra R, Yiqi Y (2011) Completely biodegradable soyprotein–jute biocomposites developed using water without any chemicals as plasticizer. *Ind Crops Prod* 33:35–41
- Ning QG, Chou TW (1995) Failure analysis of composite laminates with free edge. *J Compos Mater* 29:2280–2285
- Padal KTB, Ramji K, Prasad VVS (2014) Thermal properties of jute nanofibre reinforced composites. *Inter J Eng Res* 3:333–335
- Ray S, Eastal A (2007) Advances in polymer–filler composites: macro to nanomater. *Manuf Process* 22:741–749
- Ray D, Sarkar BK, Basak RK, Rana AK (2002) Study of the thermal behavior of alkali-treated jute fibers. *J Appl Polym Sci* 85:2594–2599
- Ray D, Sengupta S, Sengupta SP, Mohanty AK, Mishra M (2007) A study of the mechanical and fracture behavior of jute–fabric–reinforced clay–modified thermoplastic starch–matrix composites. *Macromol Mater Eng* 292:1075–1084
- Saadatmanesh H, Tavakkolizadeh M, Mostofinejad D (2010) Environmental effects on mechanical properties of wet lay-up fibre-reinforced polymer. *ACI Mater J* 107:267–274
- Satyanarayana KG, Sukumaran K, Mukherjee PS, Pavithran C, Pillai SGK (1990) Natural fibre-polymer composites. *J Cem Concr Compos* 12:117–136
- Sichina WJ (2000) Characterization of epoxy resins using DSC, Perkin Elmer Instruments. [https://shop.perkinelmer.com/Content/applicationnotes/app\\_thermalepoxyresinsusingdsc.pdf](https://shop.perkinelmer.com/Content/applicationnotes/app_thermalepoxyresinsusingdsc.pdf)
- Sing MB, Gupta M, Verma A (1995) Mechanical behaviour of particulate hybrid composite laminates as potential building materials. *Constr Build Mater* 9:39–44
- Singh RP, Zhang M, Chan D (2002) Toughening of a brittle thermosetting polymer: effects of reinforcement particle size and volume fraction. *J Mater Sci* 37:781–788
- Takagi H, Kako S, Kusano K, Ousaka A (2007) Effect of microstructure on multifunctional properties of natural fiber composites. *Adv Compos Mater* 16:377–384
- Tanoglu M, McKnight SH, Palmese GR, Gillespie JW (1998) Use of silane coupling agents to enhance the performance of adhesively bonded alumina to resin hybrid composites. *Int J Adhes* 18:431–434
- Van de V, Kiekens P (2002) Thermal degradation of flax: the determination of kinetic parameters with thermogravimetric analysis. *J Appl Polym Sci* 83:2634–2643
- Verma LS, Shrotriya AK, Singh R, Chaudhary DR (1991) Characterization of polyester films used in capacitors. I. Transient and steady-state conductivity. *J Phys D Appl Phys* 24:1729–1734
- Victor MFE, Arun S (2003) Fabrication, characterization, and dynamic behaviour of polyester/TiO<sub>2</sub> nano composites. *Mater Sic Eng A* 361:358–366
- Zou M, Boming Yu, Zhang D, Ma Y (2003) Transactions of the ASME, 125: 980–986

**Publisher's Note** Springer Nature remains neutral with regard to jurisdictional claims in published maps and institutional affiliations.